

Liouville foliation of topological billiards in the Minkowski plane.

E. E. Karginova

Moscow, department of mechanics and mathematics, MSU

Abstract.In the paper we give the Liouville classification of (we classify in the Liouville sense) five interesting cases of topological billiards glued from two flat billiards bounded by arcs of confocal quadrics in the Minkowski plane. For each billiard we calculate the marked Fomenko-Zieschang molecule, in other words the invariant of an integrable Hamiltonian system that completely determines the type of its Liouville foliation.

Keywords: Integrable system, billiard, Minkowski plane, Liouville equivalence, Fomenko-Zieschang invariant.

1 Introduction

1.1 History of the problem

A mathematical billiard is a system in which a material point (ball) moves on a planar domain bounded by a piecewise smooth curve. There are many papers devoted to integrability of such a system for different types of the boundary. Integrability of the billiard in an ellipse in the Euclidean plane was proved in the work of G. Birkhoff [1]. It is also integrable for a piecewise smooth boundary consisting of confocal quadrics such that angles between boundary arcs are not greater than $\frac{3\pi}{2}$ (i.e. they equal $\frac{\pi}{2}$ since confocal quadrics always intersect at the right angle). V.V. Kozlov and D.V. Treshchev in [4] pointed out the existence of an additional (another) independent first integral for such systems, which means they are completely/well Liouville integrable.

V.Dragovic and M.Radnovich ([23, 24]) and V.V.Fokicheva gave a full Liouville classification of flat billiards bounded by arcs of confocal quadrics. Then V.V.Fokicheva [5] considered a topological billiard glued from boundaries that are planar along arcs.

The theory of billiards was further developed by A.T.Fomenko and V.V.Vedyushkina in [18, 19, 20].

The billiard in an ellipse in the Minkowski plane was studied by V.Dragovic and M.Radnovich in [3], who described the trajectories of the system and constructed the marked molecule, i.e. the Fomenko-Zieschang invariant for the Liouville foliation of the billiard.

Earlier we introduced the definition of elementary billiards in the Minkowski plane, classified them, stated and proved the theorem of existence of only three distinct Liouville foliations for isoenergy surfaces of such billiards.

In this paper we define the topological billiard bounded by arcs of confocal quadrics in the Minkowski plane, give a number of interesting examples of such billiards as well as calculate the Fomenko-Zieschang molecule, a graph with integer marks that completely characterizes the topology of the Liouville foliation of an isoenergy surface up to the Liouville equivalence.

We express our gratitude to A.T.Fomenko for posing the problem and attention, and to V.V. Vedyushkina for consultation and valuable advice.

This paper was supported by the President program “Leading Scientific Schools” (grant no.NSh-6399.2018.1).

1.2 Some facts about the Minkowski plane

Definition 1 *The Minkowski plane is the plane \mathbb{R}^2 with the scalar product $\langle x, y \rangle = x_1y_1 - x_2y_2$.*

The distance between two points is defined by the formula $dist(x, y) = \sqrt{\langle x - y, x - y \rangle}$.

Since the scalar product can be negative, there are three disjoint sets of vectors.

Vector v is called

- *space-like* if its length is real, i.e. $\langle v, v \rangle > 0$;
- *time-like* if its length is purely imaginary, i.e $\langle v, v \rangle < 0$;
- *light-like* or isotropic if it has zero length, i.e. $\langle v, v \rangle = 0$.

Two vectors are called orthogonal if their scalar product is zero (in the Minkowski sense). It is obvious that light-like vectors are orthogonal.

Let us show how vectors of each type are located in the Minkowski plane for the origin of coordinates (fig. 1). Light-like vectors lie along two straight lines called isotropic which divide the plane into four parts. The upper and lower domains contain vectors with imaginary length, while vectors with real length are located in the right and left domains.

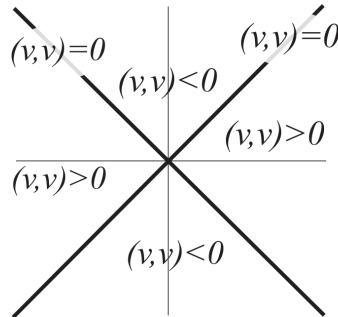


Figure 1: Different types of vectors in the Minkowski plane

1.3 Family of confocal quadrics in the Minkowski plane

In the Minkowski plane let us consider an ellipse \mathcal{E} defined by

$$\mathcal{E}: \frac{x^2}{a} + \frac{y^2}{b} = 1$$

Here $a > b > 0$, $\lambda \in \mathbf{R}$ are real numbers. The confocal family of quadrics \mathcal{C}_λ is defined by the equation:

$$\mathcal{C}_\lambda: \frac{x^2}{a-\lambda} + \frac{y^2}{b+\lambda} = 1 \tag{1}$$

The family is shown in Fig. 2.

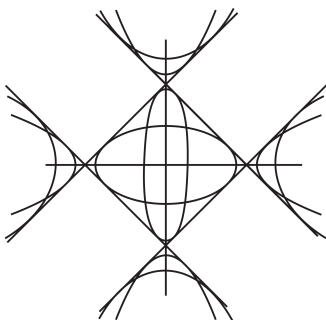


Figure 2: The family of confocal quadrics \mathcal{C}_λ in the Minkowski plane

Depending on the value of λ a quadric can be a straight line, ellipse or hyperbola. Namely,

- for $\lambda \in (-\infty, -b)$ the quadric is a hyperbola with the major axis x ;
- for $\lambda \in (a, \infty)$ the quadric is a hyperbola with the major axis y ;
- for $\lambda \in (-b, a)$ the quadric is an ellipse.

The values $\lambda = a, -b, \infty$ correspond to the degenerate quadrics $\mathcal{C}_a, \mathcal{C}_{-b}$ which are y -axis, x -axis and a straight line at infinity, respectively.

Assertion 1 *All nondegenerate quadrics of the family (1) have four common tangents, namely $x \pm y = \pm\sqrt{a+b}$.*

Assertion 2 *The family (1) has four foci, namely $F_1 = (-\sqrt{a+b}, 0), F_2 = (\sqrt{a+b}, 0), G_1 = (0, -\sqrt{a+b}), G_2 = (0, \sqrt{a+b})$. A part of an ellipse (hyperbola) whose tangent vectors are real is called a real part an ellipse (hyperbola), while that whose tangent vectors are imaginary is called an imaginary part.*

For an ellipse with parameter λ the sum of distances from the foci F_1, F_2 to any point of the real part is $=2\sqrt{a-\lambda}$, and that from G_1, G_2 to any point of

the imaginary part is $2i\sqrt{b+\lambda}$. For a hyperbola with parameter λ the difference of distances from the foci F_1, F_2 to any point of the real part of the hyperbola is $2\sqrt{a-\lambda}$, and that from G_1, G_2 to any point of the imaginary part is $2i\sqrt{b+\lambda}$.

Fig.3 shows how common tangents and foci are located relative to the family of quadrics.

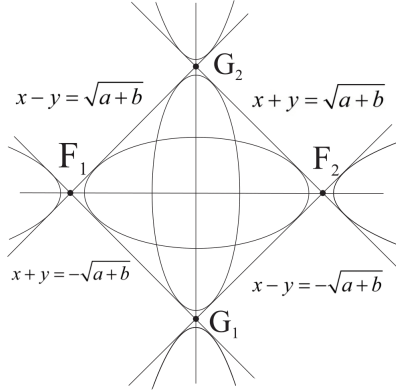


Figure 3: Relative location of common tangents and foci and a family of quadrics

It is easy to see that if two quadrics of a family intersect at some point, then the tangent vectors to the quadrics are orthogonal at this point in the Minkowski sense.

1.4 Billiard law??? in the Minkowski plane

Definition 2 Let v be a vector and ℓ be a line. We represent the vector in the form $v = v_n + v_\ell$, where v_n is the normal component of the velocity vector and v_ℓ belongs to ℓ . Then we call the vector $v' = -v_n + v_\ell$ the billiard reflection of v off the line ℓ in the Minkowski plane.

For a light-like vector v_ℓ the reflection is not defined.

We see that the scalar product of a vector by itself is preserved when using such a definition, which implies that the type of a vector does not change after reflection.

Definition 3 A line ℓ' is called the billiard reflection of ℓ off a smooth curve \mathcal{S} in the Minkowski plane if

- the intersection point A of these lines lies on the curve \mathcal{S} ;
- the directing vectors of the lines are billiard reflections of each other with respect to the tangent e to \mathcal{S} at the point A .

If the directing vector e is light-like, then the billiard reflection of the vector and line is not defined.

Note that the definition is symmetrical: if a line ℓ_1 is the billiard reflection of ℓ_2 , then the line ℓ_2 is the billiard reflection of ℓ_1 .

2 Elementary billiards in the Minkowski plane

2.1 Definition of an elementary billiard. The first integral of motion.

Definition 4 *An elementary billiard Ψ is a connected compact subset of the Minkowski plane whose boundary is a piecewise smooth curve consisting of arcs of quadrics of the family (1) that pairwise intersect at angles not greater than π .*

Note that not only the motion but also the domain in which it takes place will be called a billiard.

At points where the tangent to the domain Ψ is light-like we can extend the billiard reflection by continuity: at this point the vector is reflected to the oppositely directed one. Such points are tangency points of one of the lines $x \pm y = \sqrt{a \pm b}$ that are common for the whole family.

Definition 5 *A phase space M^4 of the billiard Ω is a 4-manifold such that*

$$M^4 = \{(x, y, v_1, v_2) | (x, y) \in \Omega, (v_1, v_2) \in T_x R^2\} / \sim$$

Equivalence relation is as follows:

$(x_1, y_1, v_1, v_2) \sim (x_2, y_2, u_1, u_2)$ if

- *$x_1 = x_2, y_1 = y_2$, the point (x_1, y_1) lies on the boundary of Ω ;*
- *$(v_1, v_2) \in l_1, (u_1, u_2) \in l_2$, and l_1 is the billiard reflection of l_2 ;*
- *$v_1^2 + v_2^2 = u_1^2 + u_2^2$ i.e. the Euclidean length of the velocity vector does not change in reflection.*

So $v_E = v_1^2 + v_2^2$ is an integral of the problem since it is the Euclidean length that is preserved for our equivalence relation.

We can take the caustic parameter λ for the trajectory as an additional integral. Simple arithmetic yields the expression of λ in terms of point coordinates in the phase space.

$$\lambda = \frac{-v_1^2 b - av_2^2 + (xv_2 - yv_1)^2}{v_1^2 - v_2^2}.$$

As is easy to see λ is preserved for reflection at a boundary point.

The integrals λ and v_e are in involution with respect to the standard Poisson brackets and are functionally independent. So for a regular part of the manifold

M^4 we can assume that the elementary billiard is Liouville integrable. This will not be used further. We will prove geometrically (without using commuting vector fields) that the regular fibers of a pair of integrals are two-dimensional tori (Liouville tori). If we restrict the system to the level surface of the integral $v_1^2 + v_2^2$, we will get a 3-manifold called isoenergy surface Q^3 , which is foliated into two surfaces when λ changes.

Definition 6 *Let v be a Liouville integrable Hamiltonian system on an isoenergy surface Q^3 . Consider the corresponding Liouville foliation on Q^3 . The base of the Liouville foliation is the space of its fibers with the standard quotient topology, i.e. the topological space whose points are considered to be fibers of the Liouville foliation (every fiber is replaced by a point).*

Definition 7 *Two Liouville integrable Hamiltonian systems v_1 and v_2 on isoenergy manifolds Q_1^3 and Q_2^3 are called coarsely Liouville equivalent if there exists a homeomorphism between the bases of the corresponding Liouville foliations that can be locally (i.e. in the neighbourhood of each point of the base) lifted up to a fiber homeomorphism of the Liouville foliations.*

Definition 8 *Let $(M_1^4, \omega_1, f_1, g_1)$ and $(M_2^4, \omega_2, f_2, g_2)$ be two Liouville integrable Hamiltonian systems on the symplectic manifolds (M_1^4, ω_1) and (M_2^4, ω_2) with the integrals f_1, g_1 and f_2, g_2 . Consider their isoenergy manifolds $Q_1^3 = \{x \in M_1^4 : f_1(x) = c_1\}$ and $Q_2^3 = \{x \in M_2^4 : f_2(x) = c_2\}$. The integrable systems are called Liouville equivalent if there exists a fiber diffeomorphism $Q_1^3 \rightarrow Q_2^3$ preserving the orientation on the 3-manifolds Q_1^3 and Q_2^3 and orientation on all critical circles.*

Theorem 1 (Fomenko-Zieschang) *Two nondegenerate integrable Hamiltonian systems on the isoenergy surfaces $Q_1^3 = \{x \in M_1^4 : f_1(x) = c_1\}$ and $Q_2^3 = \{x \in M_2^4 : f_2(x) = c_2\}$ are Liouville equivalent if and only if their marked molecules coincide.*

This theorem holds for smooth integrable systems. In our case the manifold Q^3 is piecewise smooth but it turns out that on it there is a Liouville foliation on 2-dimensional tori and special integral fibers???. Consequently, the Fomenko invariants are well-defined and we will calculate them.

2.2 Classification of elementary billiards in the Minkowski plane.

The definition of an elementary billiard was given in Section 2.1

Common tangents of the family of confocal quadrics divide the plane into several domains, five of which contain confocal ellipses or hyperbolae. We denote these domains by I, II, III, IV, and V as shown in Fig.4.

Definition 9 *An elementary billiard is called elliptical if its boundary consists of arcs of confocal ellipses and possibly parts of coordinate axes; it is called*

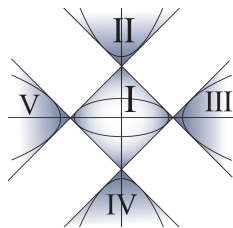


Figure 4: Domains I, II, III, IV, and V in the plane.

hyperbolic if its boundary consists of arcs of confocal hyperbolae and possibly parts of coordinate axes.

Note that in our case there is no elementary billiard whose boundary consists of arcs of both ellipses and hyperbolae since they are located in different domains of the plane (domain I contains only ellipses while hyperbolae are in II, III, IV, and V).

On the boundary of each domain there are points at which when hitting them a material point continues to move in the opposite direction. At such points there is no smoothness (intersection of boundary quadrics) or they are tangency points of the boundary and one of the common tangents.

Definition 10 *Such points split the boundary into parts called segments.*

Definition 11 *Two elementary billiards Ω and Ω' are called equivalent if one can be obtained from the other*

- *by reflection in the x -axis, y -axis or rotation by $\pi/2$ (reflection and rotation are Euclidean)*
- *by changing the parameter λ of a boundary segment (except λ corresponding to a and $-b$) so that (after changes) λ does not take values a , $-b$ and ∞ .*

Further we will speak of reflection and rotation as Euclidean ones.

Definition 12 *The boundary of an elementary billiard contains only four segments which are called *upper*, *lower*, *left*, and *right* according their location inside//within //relative to the interior of the billiard.*

Theorem 2 *Any elementary elliptical billiard is equivalent to one of the billiards in Fig.5.*



Figure 5: Classification of elementary elliptical billiards in the Minkowski metric.

3 Topological billiard in the Minkowski plane.

3.1 Definition of a topological billiard bounded by arcs of confocal quadrics in the Minkowski plane.

Definition 13 Let l_1 and l_2 be the same ??? convex or straight boundary segments of elementary billiards Ψ_1 and Ψ_2 , i.e. l_1 and l_2 belong to the same quadric of the same family of confocal quadrics. We define gluing of elementary billiards along the segments l_1 and l_2 as gluing along l_1 and l_2 by the identity isometry. Images of l_1 and l_2 after gluing are called the spine???//edge of gluing, the boundaries of the spine//edge of gluing are called the vertices of gluing???

Edges that are not edges// spines of gluing are called free edges???

Segments that have a common vertex are called adjacent.

Definition 14 A topological billiard Δ is a two-dimensional orientable manifold obtained by gluing several elementary billiards. We require that the following conditions should hold: the vertex of gluing is common for either the edge??? of gluing and two free??? edges or two edges of gluing??? (such vertices are called conical points) or four edges??? of gluing (such vertices are called inner???/internal).

In this paper we only deal with topological billiards obtained by gluing two equivalent elementary billiards.

Now we will describe the law of reflection for the topological billiard.

After gluing the law of reflection for free??? edges is the same as that for an elementary billiard. For an edge??? of gluing the law is as follows: a point continues to move on another sheet???, the line of motion is the billiard reflection of the line that the point moved along before hitting, the square of the Euclidean length of the velocity does not change.

The case of conical points should be discussed in detail. Reflection at???to??? a conical point is defined by continuity, namely, when hitting it a material point continues to move in the same domain in the opposite direction.

For this reflection??mapping??? the integral (the square of the Euclidean velocity) $v_E = v_1^2 + v_2^2$ is preserved as well as the caustic parameter λ as in the case of elementary billiards. Indeed, when we defined gluing we noted that all boundary segments belong to the same family of confocal quadrics.

Since these integrals are functionally independent and are in involution with respect to the standard Poisson bracket, we consider the system of a topological

billiard to be piecewise Liouville integrable. For detailed definitions we refer the reader to the work by V.V. Fokicheva [5].

Let us introduce an equivalence relation.

Definition 15 *A topological billiard $\Delta(2\Psi_i)$ is called equivalent to a topological billiard $\Delta'(2\Psi'_i)$ if they are obtained from each other by replacing elementary billiards with billiards equivalent to them.*

We will denote such topological billiards by $\Delta(2\Psi_i)_p^s$, where s stands for the number of glued boundary segments, namely, 1,2,3 or 4, and p stands for the number of glued straight segments. By primes in superscripts we denote the number of intersections of convex boundary segments with the coordinate axes.

4 Examples of topological integrals in the Minkowski plane.

4.1

Let us consider the following topological billiards $\Delta(2\Psi_3)_2^2$, $\Delta(2\Psi_5)^{3'}$, $\Delta(2\Psi_5)^2$, $\Delta(2\Psi_5)_1^3$, and $\Delta(2\Psi_3)_1^2$.

We state the theorem that we will prove later.

Theorem 3 *The Fomenko-Zieschang invariants for the topological billiards $\Delta(2\Psi_3)_2^2$, $\Delta(2\Psi_5)^{3'}$, $\Delta(2\Psi_5)^2$, $\Delta(2\Psi_5)_1^3$, and $\Delta(2\Psi_3)_1^2$ are shown in Fig.6.*

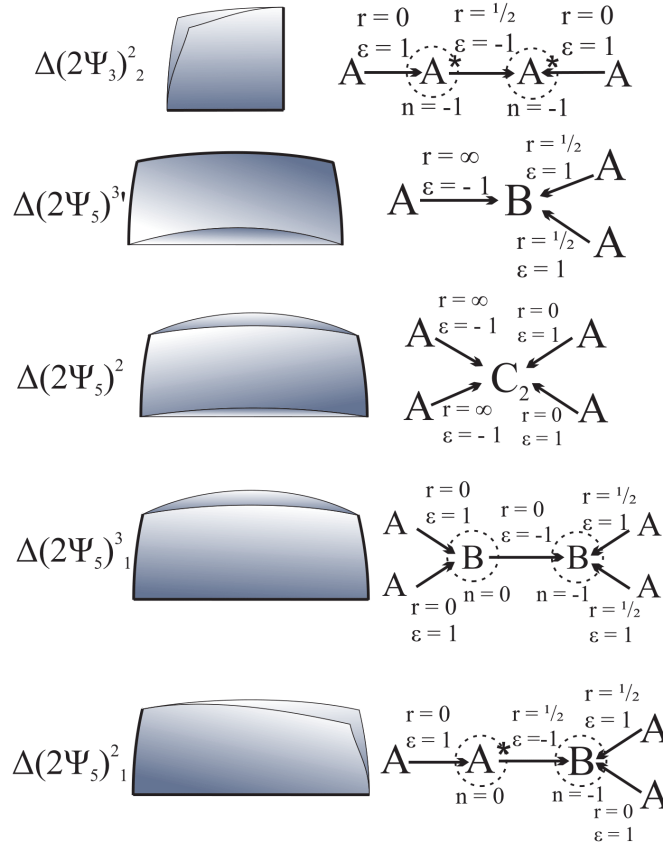


Figure 6: The Fomenko-Zieschang invariants for the specified topological billiards. The type of the billiard is in the left column, its picture is in the middle, the corresponding marked molecule is in the right column.

4.2 Singular and nonsingular levels of an integral.

Consider a topological integral $\Delta(2\Psi_i)$ obtained by gluing two elementary billiards Ψ_i . If we restrict the phase space M^4 to the level surface of the integral v_E , we will have a 3-manifold Q^3 , which is called an isoenergy surface. Changing values of the additional integral λ , we will get a foliation of the isoenergy manifold Q^3 .

Now we will define singular and nonsingular levels of the integral λ .

Definition 16 *Convex boundary values are the values of the integral λ corresponding to boundary segments that are convex relative to the interior of some domain Ψ_i . If the interior of the domain Ψ_i intersects a degenerate quadric with parameter λ equal to a or $-b$ (the quadric coincides with the y -axis or x -axis, respectively), then the corresponding value of the integral is called saddle. If gluing is defined/performed on a straight segment corresponding to the quadric parameter $\lambda = -b$ (or $\lambda = a$), then the level of the integral $\lambda = -b$ (or $\lambda = a$) is also called saddle.*

Singular values of the integral λ are by definition convex boundary and saddle values, the other values are called nonsingular.

Now we will describe trajectories lying on singular levels of the integral.

Limit trajectories on the convex boundary values of the integral are periodic (motion ?) along this segment. On a convex boundary level of the integral there may be nonsingular trajectories (when the billiard is nonsymmetrical and the image of the boundary value of the integral contains the motion within the domain formed by the boundary and the convex boundary value).

Note that when a material point hits a boundary point of a boundary segment, i.e. a point of nonsmoothness or tangency for one of common tangents, the velocity vector is identified with the vector that has the same Euclidean length/speed and opposite direction.

So limit trajectories can be different for the same boundary value of the integral λ . This is possible if several boundary segments belong to the same quadric of a confocal family. That is why we introduce the notation $\lambda = \pm bord$, where the sign $+$ is used when limit trajectories are obtained as the value of the integral λ tends to the boundary value $\lambda = bord$ from the right (the limit trajectories are time-like), and the sign $-$ is used for the limit from the left (the limit trajectories are space-like).

Preimages of such trajectories on the isoenergy surface Q^3 are a union of circles.

Trajectories on the saddle level of the integral λ belong to one of the three disjoint families: the periodic trajectory whose tangent coincides with the degenerate quadric with parameter λ equal to the saddle value of the integral, and two sets of homoclinic trajectories located on opposite sides of the periodic trajectory. Such trajectories have the focal property: at any instant a trajectory lies on a straight line passing through one of the foci (for $\lambda = -b$ the foci lie on the x -axis, for $\lambda = a$ they lie on the y -axis), moreover, the focus changes for another one when the trajectory is reflected off the boundary.

Preimages of saddle trajectories on the isoenergy manifolds are described in detail in Section 4.3.

4.3 The prototypes of singular levels of the integral: saddle values.

Let us describe the prototypes of the saddle values of the integral for such topological billiards.

Assertion 3 *The three-dimensional prototype of a small neighbourhood of the saddle value of the integral in the isoenergy surface Q^3 of topological billiards is homeomorphic to the following manifolds:*

- *an atom B for:*
 - $\Delta(2\Psi_5)^{3'}$ (saddle value $\lambda = a$),
 - $\Delta(2\Psi_5)_1^3$ (saddle value $\lambda = -b, a$),
 - $\Delta(2\Psi_5)_1^2$ (saddle value $\lambda = a$);
- *atom A^* for:*
 - $\Delta(2\Psi_3)_2^2$ (saddle value $\lambda = -b, a$),
 - $\Delta(2\Psi_5)_1^2$ (saddle value $\lambda = -b$);
- *atom C_2 for $\Delta(2\Psi_5)^2$ (saddle value $\lambda = a$).*

Proof.

1. Let's consider the billiard $\Delta(2\Psi_3)_2^2$. It is derived from two items of Ψ_3 glued together along vertical segments. Let's first glue the vertical segments, and see how the surface of the level of the singular values of the integral λ will change. Let's describe the algorithm for the level of the integral $\lambda = a$. Let's consider the tori T^u and T^d : the levels of the integral $\lambda = a$ in the isoenergy Q^3 surfaces for two billiards Ψ_3 . On each of these tori there is a cycle formed by points of vertical straight segments, equipped with vectors (these are vectors v_1 , which coincides with the vector v_4 , and v_2 , coinciding with v_3). We cut the tori into these cycles and glue them together according to the law of reflection in topological billiards, namely: $(x, v_1)_u$ sticks together with $(x, v_4)_d$, $(x, v_2)_u$ sticks together with $(x, v_3)_d$ and so on. Let's further identify two selected cycles. We will get a singular layer of atom B .

Now let's make the gluing along straight horizontal segments. In this case, a special layer of the atom B is first cut along the cycle, transversal to a singular circle, which is formed by the prototypes of points of a lower segment. Vectors were glued together along it on the lower segments on the top and bottom sheets: v_1 with v_2 , v_3 with v_4 . After the cut, the cycles are glued together in accordance with the law of reflection: the points

$(x, v_1)_u$ are identified with $(x, v_4)_d$ and vice versa, $(x, v_3)_u$ with $(x, v_2)_d$ and vice versa. Thus, a singular layer of atom B is "twisted." As a result, we obtain a special layer of the atom A^* . For the level of the integral $\lambda = -b$, the proof is similar.

2. Let's consider the billiard $\Delta(2\Psi_5)_1^2$. It is obtained by gluing together two simple billiards Ψ_5 along the left and straight lower boundary segments. First, we glue along the bottom segment.

Let's consider two tori: T^u and T^d , which lie on the level of the integral $\lambda = -b$ in Q^3 isoenergy surface. Here, similar to point 1, we obtain a special layer of atom B . Let's consider two atoms B - levels of saddle value of the integral $\lambda = a$ in the Q^3 isoenergy manifold of upper and lower billiards Ψ_5 .

Let's cut the special layers of B atoms into cycles, which are the prototypes of points lying on the lower segments of billiards Ψ_5 . Such cycles are transversal to special circles of atoms B . Vectors on the lower segments are identified along them: v_1 with v_2 and v_3 with v_4 on the upper and lower sheets. After the cut we glue what was obtained in accordance with the law of reflection: $(x, v_1)_u$ glued to $(x, v_2)_d$ and vice versa, $(x, v_3)_u$ glued to $(x, v_4)_d$ and vice versa. We get a special layer of atom B .

Now let's make a glue along the left segment. At the level of the integral $\lambda = -b$ we obtain a singular layer of atom A^* (similar to point 1) from the singular layer of atom B . At the level of the integral $\lambda = a$ after the first glue the atom B was obtained. Now let's cut a singular layer of this atom along a cycle parallel to a singular circle, which is a prototype of boundary left segment points. Along this cycle, the vectors v_4 were identified with v_1 and the vectors v_3 with v_2 on the upper and lower sheets.

Let's further glue the result in accordance with the law of reflection in topological billiards: we stick $(x, v_2)_d$ together with $(x, v_1)_u$ and vice versa, we stick $(x, v_3)_u$ together with $(x, v_2)_d$ and vice versa. Again, we obtain a special layer of atom B .

3. Let's consider now the billiard $\Delta(2\Psi_5)^2$. It is derived from two simple billiards Ψ_5 by identifying the left and right segments. We firstly glue left segments. Let's consider two atoms B , each of which is the level of the integral $\lambda = a$ in the isoenergy surface Q^3 for the upper and lower billiards Ψ_5 . Let's cut the singular layers of atoms B in cycles parallel to a singular circle that are the prototypes of left segments' points. The vectors v_1 were identified with v_4 and v_2 with v_3 on the upper and lower sheets along these cycles. Now let's glue the result in accordance with the law of reflection in the topological billiards, namely: $(x, v_1)_u$ glues with $(x, v_4)_d$, $(x, v_2)_u$ glues with $(x, v_3)_d$ and so on. We obtain a special layer of atom B_2 .

Now we glue right segments. At the same time, at the level of the integral $\lambda = a$, a singular layer of atom v is cut along the cycles parallel to a

singular circle. These cycles are the prototypes of points lying on the right segments. These vectors were previously identified along these cycles: v_1 with v_4 and vectors v_2 with v_3 on the top and bottom sheets. Let's glue the result of the cut in accordance with the billiard reflection, namely: $(x, v_1)_u$ we glue together with $(x, v_4)_d$ and vice versa, $(x, v_2)_u$ with $(x, v_3)_d$ and vice versa. Now we have a special layer of an atom C_2 . Please note, that the level of the integral $\lambda = -b$ is not singular for a given billiard

4. Let's consider the billiard $\Delta(2\Psi_5)_1^3$. It is derived from the $\Delta(2\Psi_5)^2$ billiard by identifying two identical free straight segments. Similarly to point 1, we get a special layer of atom B at the level of the integral $\lambda = -b$.

This billiard can also be derived from $\Delta(2\Psi_5)_1^3$ by identification of two right edge segments. Let's refer to the second part of point 2. While gluing the left segments a singular layer of atom B was obtained at the level of the integral $\lambda = a$ from a singular layer of atom B through the cut of the latter along a cycle parallel to the singular circle.

Now we need to make two cuts in the cycles, which are the prototypes of the left and right segments, and re-glue the result in accordance with the law of reflection in topological billiards. Obviously, we get a singular layer of atom B .

5. Let's consider the billiard $\Delta(2\Psi_5)^{3'}$. It is derived from the $\Delta(2\Psi_5)^2$ billiard by identifying two upper segments.

Let's consider the level $\lambda = a$. For that we will turn to point 4, in which the billiard $\Delta(2\Psi_5)_1^3$ was obtained from $\Delta(2\Psi_5)^2$ billiard by identifying two identical free straight segments. At the level of the integral $\lambda = a$ there is a cut of a singular layer of C_2 atom along the cycle, transversal to a singular circumference, and the subsequent gluing in accordance with the billiard law. We have shown that there is a special layer of atom B at the level of the integral $\lambda = a$. Thus, the sequence of actions described above allows us to get a singular layer of the atom B from a singular layer of the atom C_2 .

In this case, the singular layer of the C_2 atom must also be first cut along a cycle that is transversal to a particular circle, points of which are the prototypes of the upper segment of the upper and lower sheets, and then we need to glue the result in accordance with the billiard law. Thus, we obtain a special layer of the atom B . Please, note that in this topological billiard the value of the integral $\lambda = -b$ is not singular.

■

4.4 Analogue of the Liouville theorem: connected regular layers are tori.

Assertion 4 *For the topological billiard $\Delta(2\Psi_i)$ the prototypes of non-singular levels of the integral are the union of two-dimensional tori*

To prove this proposition, we will prove the following lemma.

Lemma 4.1 *For the topological billiard $\Delta(2\Psi_i)$ with $\lambda \in (-\infty, -b) \cup (a, +\infty)$ the prototypes of the non-singular levels of the integral are the union of two-dimensional tori, and if one or two adjacent or three edges are glued together, then at a fixed level of the integral λ in the isoenergy manifold Q^3 there is one torus, and if two opposite or four edges are glued together, then there are two tori.*

Proof.

Let a topological billiard consist of two items of a simple billiard Ω (which is one of the billiards $\Psi_i, i \in 1, 2, 3, 4, 5, 6$), glued along one boundary segment. Without decreasing of generality, we believe that this segment is the upper one.

We fix the value of λ belonging to the indicated interval. Let's consider the part of the billiard where the points on the level of integral of λ are projected to. Since the quadrics corresponding to the values of λ from the specified interval are hyperbolas or a line at infinity, then they do not intersect ellipses on the Minkowski plane. Therefore, the surface projection of the level of such integral values will be the exact two items of billiard Ω .

4 velocity vectors v_i correspond to each point of the billiards (x, y) , so that the point (x, y, v_i) lies at the corresponding level of the integral. Velocity vectors will be distinguished by the direction (in the 7 there are 4 types of different vectors). We obtain 8 items of billiards Ω , responsible for the upper and bottom sheets of the topological billiard, equipped with one of 4 velocity vectors. Let's denote them by $(\Omega^j, v_i)_1$ and $(\Omega^j, v_i)_2$, where i takes the values 1,2,3,4, and j takes the values 1 and 2. Let's glue these 8 items of billiard areas along the boundary according to the law of reflection in topological billiards, and thus we describe the layer of the integral λ in the isoenergy manifold Q_3 .

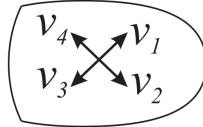


Figure 7: The direction of the velocity vectors v_1, v_2, v_3, v_4 in the billiard Ω .

Let's see how vectors on the border of the billiard are identified.

We identify v_1 with v_2 , and v_3 with v_4 in an arbitrary simple billiard on the lower and upper segments in accordance with the law of reflection. On the left and right segments we identify v_1 with v_4 , and v_2 with v_3 .

After the gluing operation on the upper segment, $v_1 \in \Omega^1$ will be identified with $v_2 \in \Omega^2$ (and, respectively, $v_1 \in \Omega^1$ will be identified with $v_2 \in \Omega^2$), and $v_3 \in \Omega^1$ with $v_4 \in \Omega^2$ (and, respectively, $v_3 \in \Omega^1$ with $v_4 \in \Omega^2$).

Therefore, we will glue the items of billiard regions (Ω^j, v_i) as follows: we glue (Ω^j, v_1) with (Ω^j, v_2) on the lower segments, and (Ω^j, v_3) with (Ω^j, v_4) (here j takes the values 1, 2), on the left and right segments we glue (Ω^j, v_1) with (Ω^j, v_4) , and (Ω^j, v_2) with (Ω^j, v_3) (here j takes values 1, 2).

On the top segment, we glue (Ω^1, v_1) with (Ω^2, v_2) , (Ω^2, v_1) with (Ω^1, v_2) , and (Ω^1, v_3) with (Ω^2, v_4) , (Ω^2, v_3) with (Ω^1, v_4) . This algorithm is shown in the Fig. 8 the identified vectors are connected by the dotted line.

Then the level of the integral is homeomorphic to 8 quadrangles glued with each other by the above rule. It's easy to see that it represents a torus.

For the remaining cases of sides gluing the proof is similar.

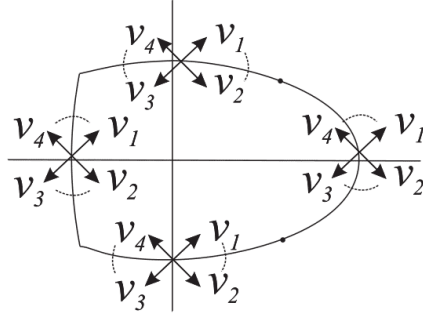


Figure 8: Identification of vectors v_1, v_2, v_3, v_4 on the billiard boundary Ω . ■

Remark 1 *Let's note that, when proving the important things are only the number of glued areas and the number of boundary segments identified with each other by gluing operation (and their location relative to each other, if there are two of such segments). Thus, let's suppose that while considering a topological billiard $\Delta(2\Psi_i)$ in the form of a non-singular value of the integral λ , the billiard motion occurs in a region with several boundary segments identified with each other. Then, we can hold a similar proof and conclude that at the appropriate level of the integral in the isoenergy surface of Q^3 there are two-dimensional tori for every such area.*

The number of tori will be the same as in Lemma 4.1, namely: when gluing one, two adjacent or three segments there will be one torus, and there are two tori when gluing two opposite or four.

Remark 2 *As it is followed from Comment 1 and Lemma 4.1, if in the prototype of the non-singular level of the integral the billiard motion occurs in a disconnected union of two regions, then at the appropriate level of the integral in an isoenergy manifold there will be two tori.*

Proof. Let's consider some topological billiard Ω , obtained by gluing together two equivalent simple billiards Ψ_i . For $\lambda \in (-\infty, -b) \cup (a, \infty)$ the assertion is proved in the lemma; therefore, we fix some value of the integral $\lambda \in (-b, a)$ which, by the definition, is non-singular (that is, it is not a boundary one).

Let's consider the level projection of the integral λ on the billiard plane and cut those parts out from the region Ω into which the level points of the integral are not projected. We obtain some billiard Ω' , possibly, disconnected. According to the algorithm described in Lemma 4.1, each connected component is glued into a union of several tori. The number of these tori depends on the number of connected components and glued segments. ■

4.5 Fomenko-Zieschang molecule - complete invariant of Liouville equivalence

So then, the description for each leave of the Liouville foliation is provided above for each of the $\Delta(2\Psi_3)_2^2$, $\Delta(2\Psi_5)^{3'}$, $\Delta(2\Psi_5)^2$, $\Delta(2\Psi_5)_1^3$ and $\Delta(2\Psi_3)_1^2$ topological billiards. Namely, it is proved that nonspecial leaves are tori, while special leaves are 3-atoms. However, to fully describe the topology of the Liouville structure, additional information regarding the way the regular neighborhoods of special leaves are glued to each other is required. Let us select permissible bases on each boundary torus and specify the transition matrix from one basis to another one. The rule for selecting permissible bases is defined by the atom structure.

Remember, that we select solid torus median on the boundary torus of the A atom as the λ cycle, that is a cycle contracting to a point inside the solid torus, while the μ cycle is to complete the basis. In this case, it is convenient to consider the μ cycle a fiber of Seifert fibration. Fibers of Seifert fibration have natural orientation defined by the Hamiltonian vector field. More specifically, one of these fibers is a trajectory of the vector field in question, namely, the critical circle of the λ additional integral, the axis of solid torus. The orientation of this fiber makes it possible to exactly determine the orientation on the μ cycle.

In case of the B saddle 2-atom, the corresponding U 3-atom has the structure of the trivial S^1 -foliation into two-dimensional B atoms (the “thickened eight”). On each of the T_i boundary tori, we take a fiber of this foliation as the λ_i cycle. We select additional μ_i cycles as follows. Let us consider arbitrary cross-section, $P \in U$. On each boundary torus T_i , it intercepts a certain μ_i cycle. It is this cycle that we take as the second basis cycle on T_i . As in the previous case, the orientation is selected uniquely.

On other saddle atoms without stars, cycles are selected in the similar way. Namely, the λ cycle is a fiber of Seifert fibration, while μ cycles are intercepted in boundary tori by cross-sectioning of a three-dimensional atom with a flat atom.

Therefore, each point of an edge has two bases, which are determined consistently with the atoms connected by the selected edge of the graph. The matrix for transition from one basis to the other one is referred to as gluing matrix. Since permissible bases are selected nonuniquely, the gluing matrix may be different when different bases are selected. However, when the gluing matrix is available, it is possible to calculate r, ε, n numerical metrics - invariants with regard to possible substitutions of bases on boundary tori (see lemmas 4.5 and 4.6 in book [2]). Detailed rules for calculating these numbers are provided in [2].

Definition 17 *A molecule provided with r, ε, n labels is referred to as labelled molecule or Fomenko-Zieschang invariant.*

4.6 Counting labels in Fomenko-Zieschang molecules for certain topological billiards on Minkowski plane

To prove the following lemmas, let us introduce the following notations. For simple billiards Ψ_3, Ψ_5, Ψ_6 (as well as for topological billiards obtained by gluing these simple billiards), the parameter of the upper (and the lower, in case it is convex) segment is λ_2 , while the parameter of the right (and the left, in case it is convex) segment is λ_1 .

Definition 18 We call the cycle orientation consistent if its orientation coincides with the orientation of the speed vectors, and inconsistent, if the cycle orientation is opposite to the orientation of the speed vectors.

Lemma 4.2 Figure 6 shows Fomenko-Zieschang invariant for the $\Delta(2\Psi_3)_2^2$ domain

Proof. Let us orient the edges of the molecule in accordance with the figure 6 - the orientation shows the from and the to basis of the transition. Let us

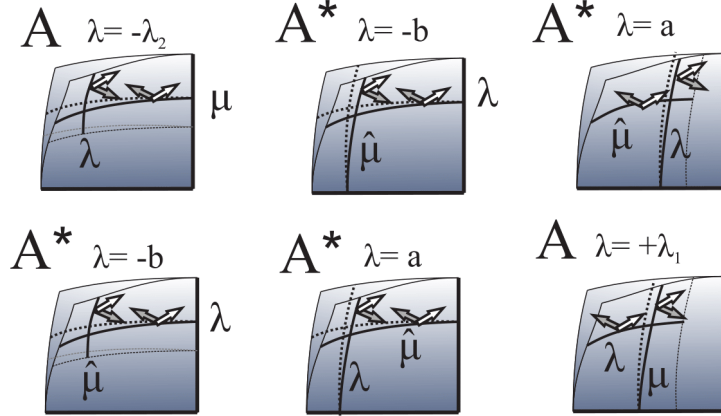


Figure 9: Selecting cycles for the $\Delta(2\Psi_3)_2^2$ domain. In the first column, cycles for the edge that corresponds to values of the $\lambda \in (-b, -\lambda_2)$ integral are selected, in the second column - to $\lambda \in (-\infty, -b) \cup (a, +\infty) \cup \{\infty\}$, in the third column - $\lambda \in (+\lambda_1, a)$. The thin dashed line specifies the arc of the integral ellipse with its orientation indicated by the white arrow on the cycle.

consider the edge that corresponds to values of the $\lambda \in (-b, -\lambda_2)$ integral.

The figure shows the selection of cycles on a boundary torus of the A atom. Indeed, when the parameter of the integral ellipse tends to the value of $\lambda = -\lambda_2$, the λ cycle contracts to a point, while the μ cycle transitions into the A atom's critical circle (moreover, its orientation is consistent with the orientation of the atom's critical circle). Now, let us describe the selection of cycles on boundary tori of the A^* atom. To begin with, we take fibers of Seifert fibration as λ

cycles (figure 9) where their orientation is consistent with that of the critical circle. Let us consider interception of the A^* 3-atom with a B atom which is transversal to the special circle. It intercepts three $\hat{\mu}$ cycles on the edge of the 3-atom with two of them intercepted on the elliptical torus and intersect the λ cycle (a Seifert fibration fiber) once, and the third one, $\hat{\mu}$, intercepted on the hyperbolic torus intersects a Seifert fibration fiber twice. Let us use such $\hat{\mu}$ cycles (shown in figure 9) to construct a true μ cycles on boundary tori of the A^* atom. For the elliptical torus of an edge, we select one of the connected $\hat{\mu}$ components as μ , while for the hyperbolic torus - the $\mu = \frac{\lambda + \hat{\mu}}{2}$ cycle.

Cycles for the A^* atom that corresponds to the $\lambda = a$ parameter are selected in the similar way (see figure 9)

And finally, cycles of the boundary torus of the A atom that corresponds to the value of the $\lambda = +\lambda_1$ parameter are shown in figure 9. These cycles are selected the same way as for the A atom that corresponds to the value of the $\lambda = -\lambda_2$ parameter.

Now, let us write down the matrices for transitioning from one basis to another one (starting from the left edge) following the previously fixed orientation of the edges.

For the left edge, the $\begin{pmatrix} 0 & 1 \\ 1 & 0 \end{pmatrix}$ gluing matrix, where the λ orientation of the A atom's boundary torus is selected based on the condition for the gluing matrix determinant, and the $\hat{\mu}$ orientation (and, apparently, the orientation of μ along with it) of the saddle atom is considered consistent. Labels on this edge are $r = 0, \varepsilon = 1$.

For the middle edge we have $\begin{pmatrix} 1 & -2 \\ 0 & -1 \end{pmatrix}$, where the orientation of $\hat{\mu}$ (defining the orientation of μ) of the A^* atom that corresponds to the value of $\lambda = a$ is selected from the condition for the determinant. Labels on this edge are $r = \frac{1}{2}, \varepsilon = -1$.

Now, the orientation of $\hat{\mu}$ for boundary tori of the saddle atom on the right edge is selected uniquely (and this orientation determines the orientation of the μ cycle). The gluing matrix is $\begin{pmatrix} 0 & 1 \\ 1 & 0 \end{pmatrix}$, the orientation of the A atom is selected from the condition for the determinant. Labels of this edge are $r = 0, \varepsilon = 1$.

We have two families in the molecule. The $n = -1$ label is for both of them (this follows from the definition and the explicit form of the gluing matrices). ■

Lemma 4.3 *figure 6 shows Fomenko-Zieschang invariant for the $\Delta(2\Psi_5)^{3'}$ domain*

Proof. We orient the edges of the crude molecule toward the saddle atom. Let us consider the edge that corresponds to values of the $\lambda \in (-\infty, -\lambda_2) \cup$

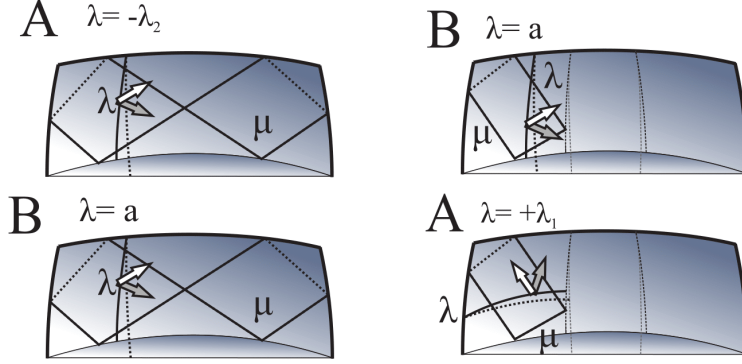


Figure 10: Selecting cycles for the $\Delta(2\Psi_5)^{3'}$ domain. In the first column, cycles for the edge corresponding to values of the $\lambda \in (-\infty, -\lambda_2) \cup (a, +\infty) \cup \{\infty\}$ integral are selected, in the second column – to $\lambda \in (+\lambda_1, a)$. The thin dashed line specifies the arc of the integral ellipse. We indicate its orientation by the white arrow on the cycle.

$(a, +\infty) \cup \{\infty\}$ integral.

Figure 10 shows the selection of cycles on boundary tori of the A atom. Indeed, when the value of the λ integral tends to the boundary value of $-\lambda_2$, the λ cycle contracts to a point. In this case, the μ cycle contracts to the critical circle of the atom, and its orientation is selected as consistent with that of the critical circle.

Figure 10 shows the selection of cycles on the B atom. Here, λ is a fiber of Seifert fibration, and its orientation is consistent with that of the critical circle, while the μ cycle is the one that is intercepted by a certain cross-section of the three-dimensional B atom by the two-dimensional B atom. Orientation of the cycle is selected as consistent. In this case, the gluing matrix on this edge is $\begin{pmatrix} -1 & 0 \\ 0 & 1 \end{pmatrix}$, whereupon, the orientation of the λ cycle for the boundary torus of the A atom is selected from the condition for the matrix determinant. In this case, the labels on this edge are $r = \infty, \varepsilon = -1$.

Now, let us consider one of the molecule edges that corresponds to the value of the $\lambda \in (+\lambda_1, a)$ parameter.

Figure 10 shows the selection of cycles on boundary tori of atoms. As a matter of fact, on the boundary torus of the B atom, the λ cycle is a fiber of Seifert fibration, and its orientation is consistent with that of the critical circle, while the μ cycle is a cross-section of the B atom's boundary torus by

the two-dimensional B atom, moreover, the orientation on it is already defined - if the orientation of the μ cycle on the outer boundary torus is consistent, it would be inconsistent on inner ones since orientations of μ cycles is bound by the condition of the global cross-section existence.

On the boundary torus of the A atom, the μ cycle is contracted to the critical circle, and its orientation is consistent with that of this circle, while the λ cycle is contracted to a point when the value of the λ integral tends to the boundary value of $+\lambda_2$. It is easy verified that $\mu_B = -\frac{\pm\lambda_A + \lambda_B}{2} = -\mu_A$ (minus since the orientation is inconsistent, and the λ_A sign is selected from the condition for the determinant of the transfer matrix). Then, the gluing matrix is $\begin{pmatrix} 1 & 2 \\ 0 & -1 \end{pmatrix}$, which means that the λ_A orientation is selected as inconsistent. In this case, the labels on this edge are $r = \frac{1}{2}, \varepsilon = 1$.

For the second edge corresponding to these values of the parameter, cycles are selected in the similar way, so, the labels are also $r = \frac{1}{2}, \varepsilon = 1$. ■

Lemma 4.4 *Figure 6 shows the Fomenko-Zieschang invariant for the $\Delta(2\Psi_5)^2$ billiard*

Proof. We orient both edges of the molecule towards the saddle atom.

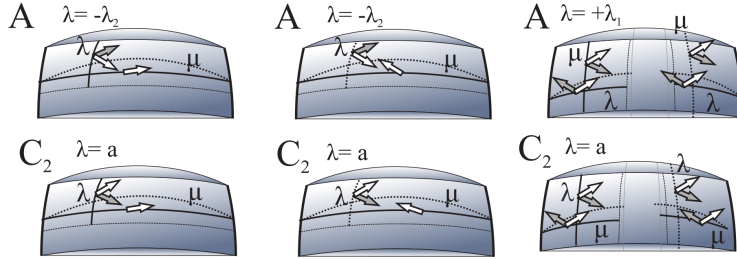


Figure 11: Selecting cycles for the $\Delta(2\Psi_5)^2$ domain. In the first column, cycles are selected for the edge corresponding to values of the $\lambda \in (-\infty, -\lambda_2) \cup (a, +\infty) \cup \{\infty\}$ integral, in the second column - to $\lambda \in (+\lambda_1, a)$. The thin dashed line specifies the arc of the integral ellipse, and the white arrow on the cycle indicates its orientation.

Let us consider the edges that correspond to values of the $\lambda \in (-\infty, -\lambda_2) \cup (a, \infty) \cup \{\infty\}$ integral.

Figure 11 shows cycles for boundary tori of A atoms. Indeed, you can easily see that when the parameter of the integral ellipse tends to the value of $\lambda = -\lambda_2$, the λ cycle contracts to a point (the orientation is not yet defined on it), while the μ cycle contracts to a special circle (moreover, its orientation is consistent with the orientation of the special circle).

Figure 11 shows cycles for boundary tori of C_2 atoms. Indeed, cycles λ contract to special circles and their orientation is selected as consistent with the

orientation of these circles, while cycles μ are intercepted on boundary tori by several cross-sections of the C_2 3-atom by the flat C_2 atom. Let us select the orientation of these cycles as consistent.

Then, the gluing matrices on the upper and lower edges are $\begin{pmatrix} -1 & 0 \\ 0 & 1 \end{pmatrix}$, (please note that now we can select the λ orientation on A atoms based on the condition for the gluing matrix determinant), whereupon the labels would be $r = \infty, \varepsilon = -1$ on both edges.

Let us consider the edges that correspond to values of $\lambda \in (+\lambda_1, a)$.

Figure 11 shows cycles for boundary tori of atoms. Indeed, on tori of the C_2 saddle atom, the λ cycles contract to special circles (and their orientation is consistent with that of the special circles), while μ cycles are intercepted on boundary tori of the C_2 saddle 3-atom by the C_2 two-dimensional atom. Since all μ cycles are related to the condition for existence of the global cross-section, the orientation of the cycles selected on these two boundary tori would be inconsistent.

On A boundary atoms, λ cycles contract to a point when the parameter of the integral ellipse tends to the value of $+\lambda_1$, and the orientation on them is defined later based on the condition for the gluing matrix determinant. μ cycles contract to special circles, and their orientation is consistent with that of the special circles.

Then, the gluing matrices are $\begin{pmatrix} 0 & 1 \\ 1 & 0 \end{pmatrix}$ for the upper and lower edges (now, we can select the orientation of λ cycles on tori of A atoms), and the labels would be $r = 0, \varepsilon = 1$ for the upper and lower edges. ■

Lemma 4.5 *Figure 6 shows Fomenko-Zieschang invariant for the $\Delta(2\Psi_5)_1^3$ biliard*

Proof. We orient edges of the molecule according to figure 6.

Let us consider the edges that correspond to values of the $\lambda \in (-b, -\lambda_2)$ integral. Figure 12 shows the selection of cycles on boundary tori of atoms. On boundary tori of A atoms, cycles are selected the same way as in lemma 4.4 for edges with similar parameters. On boundary tori of the B , λ cycles contract to a special circle, and their orientation is defined by the orientation of the critical circle, while μ cycles represent the cross-section of the B 3-atom by the B 2-atom and their orientation is considered consistent. In this case, the gluing matrix for both edges is $\begin{pmatrix} 0 & 1 \\ 1 & 0 \end{pmatrix}$, and the labels on these edges are $r = 0, \varepsilon = 1$

Let us consider the edge that corresponds to values of the $\lambda \in (-\infty, -b) \cup (a, \infty) \cup \{\infty\}$ integral. Figure 12 shows the selection of cycles. On the boundary torus of the B atom that corresponds to the value of the $\lambda = -b$ parameter, the μ_- cycle (its orientation has already been fixed and is inconsistent) and the λ_- cycle (it contracts to a special circle of the atom, and its orientation is consistent with that of the circle) are selected.

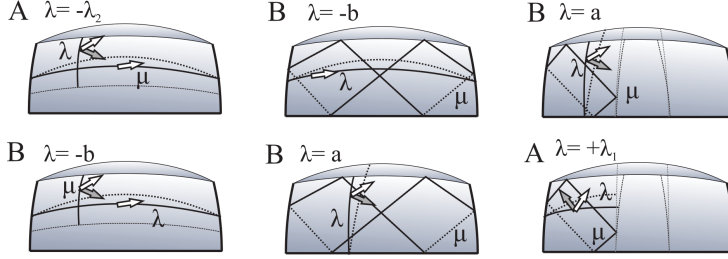


Figure 12: Selecting cycles for the $\Delta(2\Psi_5)_1^3$ domain. In the first column, cycles are selected for the edge that corresponds to values of the $\lambda \in (-b, -\lambda_2)$ integral, in the second column - to $\lambda \in (-\infty, -b) \cup (a, +\infty) \cup \{\infty\}$, in the third column - to $\lambda \in (+\lambda_1, a)$. The thin dashed line specifies the arc of the integral ellipse, the white arrow on the cycle indicates its orientation.

On the boundary torus of the B atom that corresponds to the value of the $\lambda = a$ parameter, the μ_+ cycle (its orientation has not been fixed yet, and this cycle is intercepted on a boundary torus by the cross-section of the B 3-atom by the B 2-atom) and the λ_+ cycle (its contracts to a special circle of the atom, its orientation is fixed and consistent with that of the circle) are selected.

It is easily verified that $\mu_+ = \pm(\lambda_+ + \lambda_-)$ (moreover, the sign is selected based on the condition for the winner of the gluing matrix and defines the consistent or inconsistent orientation of the μ_+ cycle). Since $\lambda_+ = -\mu_-$ (remember that the orientation of μ_- is inconsistent), the gluing matrix is $\begin{pmatrix} 0 & -1 \\ \pm 1 & \mp 1 \end{pmatrix}$. Since the determinant of this matrix must be equal to -1, we finally conclude that the matrix is $\begin{pmatrix} 0 & -1 \\ 1 & -1 \end{pmatrix}$, the orientation of μ_+ is inconsistent, and the labels on the edge are $r = 0, \varepsilon = -1$.

Let us consider the edges that correspond to values of the $\lambda \in (+\lambda_1, a)$ integral. Figure 12 shows the selection of cycles on boundary atoms.

On boundary tori of the B atom, μ_+ cycles are intercepted by the B 2-atom and their orientation is fixed and consistent, while λ_+ cycles represent a fiber of Seifert fibration, and their orientation is consistent with the orientation of the atom's critical circle

On boundary tori of the A atom, the λ_- cycle contracts to a point when the parameter of the integral ellipse tends to the value of $+\lambda_1$, while the μ_- cycle contracts to a special circle of the atom with its orientation defined by that of this circle. It is easily verified that $\mu_- = \frac{\pm\lambda_- + \lambda_+}{2} = \mu_+$. We orient λ_- logically based on the condition for the determinant of the gluing matrix. Then, the gluing matrices for the upper and lower edges are $\begin{pmatrix} -1 & 2 \\ 0 & 1 \end{pmatrix}$, while the labels on both edges are $r = \frac{1}{2}, \varepsilon = 1$.

So then, there are two families in the molecule. For the left one, the label is $n = 0$, for the right one, the label is $n = [-\frac{-1}{1}] + [-\frac{1}{2}] + [-\frac{1}{2}] = -1$ (it follows from the definition and explicit form of the gluing matrices for each edge). ■

Lemma 4.6 *Figure 6 shows the Fomenko-Zieschang invariant for the $\Delta(2\Psi_3)_1^2$ domain*

Proof. We orient the edge according to figure 6.

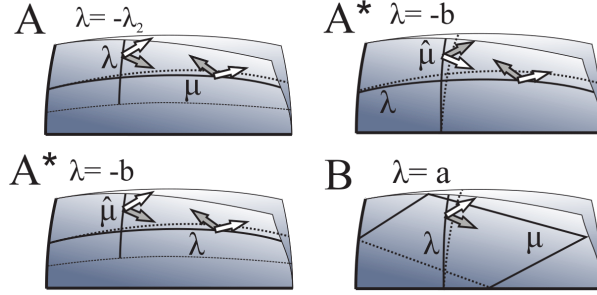


Figure 13: Selecting cycles for the $\Delta(2\Psi_3)_1^2$ domain. In the first column, cycles are selected for the edge that corresponds to values of the $\lambda \in (-b, -\lambda_2)$ integral, in the second column - to $\lambda \in (-\infty, -b) \cup (a, +\infty) \cup \{\infty\}$. The thin dashed line specifies the arc of the integral ellipse, the white arrow on the cycle indicates its orientation.

Let us consider the edge that corresponds to values of $\lambda \in (-b, -\lambda_2)$. Figure 13 shows the selection of cycles for boundary atoms. On a boundary torus of the A atom, the λ cycle contracts to a point when the parameter of the integral ellipse tends to $-\lambda_2$ (the orientation of this cycle is defined later when writing the gluing matrix), the μ cycle contracts to the critical circle of the atom with its orientation being consistent.

On a boundary torus of the A^* atom, the λ cycle is a fiber of Seifert fibration and its orientation is consistent with that of the special circle of the atom. Let us describe the selection of the μ cycle.

Let us consider cycles intercepted on boundary tori of the A^* 3-atom by the B two-dimensional atom. There are 3 $\hat{\mu}$ cycles with two of them intercepted on the elliptical torus, and the third one is intercepted on the hyperbolic torus and crosses the highlighted fiber of Seifert fibration twice. To construct true μ cycles, on the elliptic torus, we take one of the connected components of $\hat{\mu}$ cycles (and choose its orientation as consistent), and $\mu = \frac{\hat{\mu} + \lambda}{2}$ on the hyperbolic torus where λ is a fiber of Seifert fibration (which means that the λ cycle on the elliptic torus is also a fiber of Seifert fibration) with the $\hat{\mu}$ orientation being inconsistent.

Then, on the edge in question, the gluing matrix is $\begin{pmatrix} 0 & 1 \\ 1 & 0 \end{pmatrix}$, and the labels are $r = 0, \varepsilon = 1$.

Let us consider the edge that corresponds to values of the $\lambda \in (-\infty, -b) \cup (a, \infty) \cup \{\infty\}$ integral. Figure 13 shows the selection of cycles on boundary tori of atoms

On a torus of the A^* atom, the λ_- cycle is a fiber of Seifert fibration, its orientation is fixed, the selection of the μ_- cycle is described above (namely, $\mu_- = \frac{\hat{\mu} + \lambda_-}{2}$)

On a torus of the B atom, the λ_+ cycle contracts to a special circle, and its orientation is consistent with that of the special circle, while the μ_+ cycle is intercepted on the elliptical torus using the cross-section of the 3-atom by the flat B atom. It is easily verified that $\mu_+ = \pm \frac{\lambda_+ + \lambda_-}{2}$.

Since $\hat{\mu} = -\lambda_+$, then the gluing matrix is $\begin{pmatrix} 1 & -2 \\ \pm 1 & \mp 1 \end{pmatrix}$. Its determinant must be equal to -1, and we select the inconsistent orientation for μ_+ . Then, the matrix is rewritten as $\begin{pmatrix} 1 & -2 \\ -1 & 1 \end{pmatrix}$, while the labels on the edge are $r = \frac{1}{2}, \varepsilon = -1$.

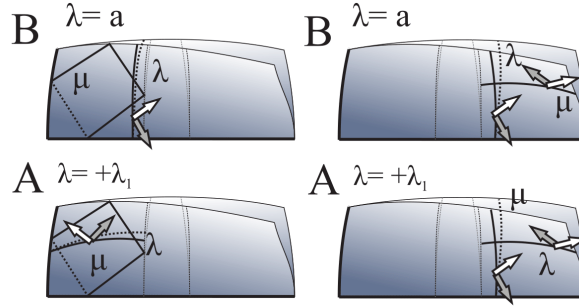


Figure 14: Selecting cycles for the $\Delta(2\Psi_3)_1^2$ domain for the edge that corresponds to values of the $\lambda \in (+\lambda_1, a)$ integral. The thin dashed line specifies the arc of the integral ellipse, the white arrow on the cycle indicates its orientation.

Let us consider the edges that correspond to values of the $\lambda \in (+\lambda_1, a)$ integral.

Projection of a torus on the billiard plane breaks into two connected components.

For the case when a connected component contains a conical point, the selection of cycles is shown in figure 14 and is performed the same way as in... Consequently, $\mu_+ = \mu_- = \frac{\lambda_+ \pm \lambda_-}{2}$. We select the orientation of λ_- so that the

gluing matrix determinant be equal to -1. The gluing matrix is $\begin{pmatrix} -1 & 2 \\ 0 & 1 \end{pmatrix}$, the

labels on the edge are $r = \frac{1}{2}, \varepsilon = 1$ For the case when a connected component does not contain conical points, the selection of cycles is shown in figure 14 On a boundary torus of the A atom, the μ cycle contracts to a special circle and its orientation is consistent with that of the circle, while the λ contracts to a point. On a boundary torus of the B atom, the orientation of the μ cycle is

consistent, while the orientation of the λ cycle (a fiber of Seifert fibration) is consistent with that of the critical circle of the atom. Then, the gluing matrix is $\begin{pmatrix} 0 & 1 \\ 1 & 0 \end{pmatrix}$, while the labels on the edge are $r = 0, \varepsilon = 1$.

There are two families in the molecule, For the left one, the label is $n = 0 + [\frac{1}{-2}] = -1$, for the right one, the label is $n = 0 + [-\frac{1}{-2}] + [-\frac{1}{2}] = -1$ (it follows from the definition and explicit form of gluing matrices for each edge). ■

References

- [1] G. D. Birkhoff, , Dynamical Systems, , Amer. Math. Soc. Colloq. Publ., vol. 9, , Amer. Math. Soc., New York , 1927
- [2] A. V. Bolsinov and A. T. Fomenko, , Integrable Hamiltonian Systems. Geometry, Topology, Classification, , vol. 1,2 , Izhevsk , Regular and Chaotic Dynamics, scientific research center , 1999
- [3] V. Dragovic and M. Radnovic , Topological Invariants for Elliptical Billiards and Geodesics on Ellipsoids , Fundamental and Applied Mathematics , 20: 3 , pp. 51–64 , 2015
- [4] V. V. Kozlov and D. V. Treshchev , A Genetic Introduction to the Dynamics of Systems with Impacts , M. , Moscow Univ. , 1991
- [5] V. V. Fokicheva , A Topological Classification of Billiards in Locally Planar Domains Bounded by Arcs of Confocal Quadrics , Mat. Sb. , 206: 10 , pp. 127–176 , 2015
- [6] A. A. Oshemkov , Invariants of the Main Integrable Cases of the Rigid Body Motion Equations , Advances in Soviet Mathematics, AMS , vol. 6 , pp. 67–146 , 1991
- [7] A. T. Fomenko , The Symplectic Topology of Completely Integrable Hamiltonian Systems , Uspekhi Mat. Nauk , vol. 44 , 1(265) , pp. 145–173 , 1989
- [8] A. T. Fomenko and H. Zieschang , A Topological Invariant and a Criterion for the Equivalence of Integrable Hamiltonian Systems with Two Degrees of Freedom , Izv. Akad. Nauk SSSR , 54: 3 , pp. 546–575 , 1990
- [9] A. T. Fomenko , A Bordism Theory for Integrable Nondegenerate Hamiltonian Systems with Two Degrees of Freedom. A New Topological Invariant of Higher-Dimensional Integrable Systems , Mathematics of the USSR-Izvestiya , 55: 4 , pp. 747–779 , 1991
- [10] A. T. Fomenko , Symplectic Geometry , Second revised edition , Gordon and Breach , 1995

- [11] S. V. Matveev and A. T. Fomenko , Algorithmic and Computer Methods for Three-Manifolds , Moscow , Science , 1998
- [12] A. T. Fomenko, P. V. Morozov , Some New Results in Topological Classification of Integrable Systems in Rigid Body Dynamics , Proceedings of the Workshop Contemporary Geometry and Related Topics”., 15-21 May 2002 , Belgrade, Yugoslavia , World Scientific Publishing Co. , 2004 , pp. 201–222
- [13] E. A. Kudryavtseva, I. M. Nikonov and A. T. Fomenko , Maximally Symmetric Cell Decompositions of Surfaces and their Coverings , Mat. Sb. , 199: 9 , pp. 3–96 , 2008
- [14] A. T. Fomenko, A. Yu. Konyaev , New Approach to Symmetries and Singularities in Integrable Hamiltonian Systems , Topology and its Applications , vol. 159 , pp. 1964–1975 , 2012
- [15] E. A. Kudryavtseva and A. T. Fomenko , Symmetries Groups of Nice Morse Functions on Surfaces , Dokl. Ross. Akad. Nauk , 446:6 , pp. 615–617 , 2012
- [16] A. T. Fomenko and A. Yu. Konyaev , Algebra and Geometry Through Hamiltonian Systems , Continuous and Distributed Systems. Theory and Applications , Solid Mechanics and Its Applications , vol. 211 , pp. 3–21 , 2014
- [17] A. T. Fomenko, S. S. Nikolaenko , The Chaplygin Case in Dynamics of a Rigid Body in Fluid is Orbitally Equivalent to the Euler Case in Rigid Body Dynamics and to the Jacobi Problem about Geodesics on the Ellipsoid , Journal of Geometry and Physics , vol. 87 , pp. 115–133 , 2015
- [18] V. V. Fokicheva and A. T. Fomenko , Integrable Billiards Model. Important Integrable Cases of Rigid Body Dynamics , RAS report, mathematics , 465: 2 , pp. 150–153 , 2015
- [19] V. V. Fokicheva and A. T. Fomenko , Billiard Systems as the Models for the Rigid Body Dynamics , Studies in Systems, Decision and Control , Advances in Dynamical Systems and Control , vol. 69 , pp. 13–32
- [20] V. V. Vedyushkina (Fokicheva) and A. T. Fomenko , Integrable Topological Billiards and Equivalent Dynamical Systems , Izv. Ross. Akad. Nauk Ser. Mat. , 81: 4 , pp. 20–67 , 2017
- [21] A. T. Fomenko, V. V. Trofimov , Integrable Systems on Lie Algebras and Symmetric Spaces , Gordon and Breach , 1988
- [22] S. V. Matveev and A. T. Fomenko , Morse-type Theory for Integrable Hamiltonian Systems with Tame Integrals , Math. Notes , 43: 5 , pp. 663–671 , 1988

- [23] V. Dragovic, M. Radnovic , Bifrucations of Liouville Tori in Elliptical Billiards , V. A. Steklov Math. Institute of RAS, Regul. Chaotic Dyn. , vol. 14, 4-5 , pp. 479–494 , 2009
- [24] V. Dragovic, M. Radnovic , Poncelet Porisms and Beyond. Integrable Billiards, Hyperelliptic Jacobians and Pencils of Quadrics , Front. Math. , Birkhauser/SpringerBasel AG, Basel , 2011